

# Near-field light emission from dark-states inverted exciton occupations

G. Pistone, S. Savasta,\* O. Di Stefano, G. Martino, and R. Girlanda  
*Dipartimento di Fisica della Materia e Tecnologie Fisiche Avanzate,  
 Università di Messina  
 Salita Sperone 31, I-98166 Messina, Italy*

Stefano Portolan  
*Dipartimento di Fisica, Politecnico di Torino, Corso Duca degli Abruzzi 24, 10129 Torino, Italy  
 (Dated: March 23, 2022)*

We theoretically analyze the carrier capture and distribution among the available energy levels of a symmetric semiconductor quantum dot under continuous-wave excitation resonant with the barrier energy levels. At low temperature all the dot level-occupations but one decrease monotonically with energy. The uncovered exception, corresponding to the second (dark) energy level, displays a steady-state carrier density exceeding that of the lowest level more than a factor two. The root cause is not radiative recombination before relaxation to lower energy levels, but at the opposite, carrier trapping due to the symmetry-induced suppression of radiative recombination. Such a behaviour can be observed by collection-mode near-field optical microscopy.

Understanding how electron-hole pairs distribute among the available energy levels of semiconductor nanostructures after optical excitation or current injection is crucial for the development of novel quantum devices [1]. One tool frequently used to explore the energy distribution of electron-hole pairs is photoluminescence spectroscopy (PL). It provides a direct measurement of the optical density of states times the excitonic population density as a function of energy. Detailed simulations of Zimmermann *et al* [2, 3] have clarified many aspects of the intriguing nonequilibrium dynamics determining the distribution of excitonic populations among the available energy levels in quantum wells (QWs) with interface roughness. Already at temperatures around 40-50 K the individual occupation of states is close to the Boltzmann distribution since all states can frequently emit and absorb phonons to reach equilibrium before radiative emission. At lower temperature more localized states displaying smaller phonon scattering rates cannot equilibrate and their occupations deviate from the Boltzmann distribution, displaying a reduced energy dependence. Far-field PL spectroscopy provide average measurements over a distribution of different emission sites. The opportunity for important insight is often lost by the inability to resolve finer details within this distribution. Scanning near-field optical microscopy (SNOM) combines the advantages of nanometric resolution of scanning-probe microscopy with the unique possibility of characterizing quantum systems offered by optical spectroscopy. The SNOM ability to resolve the individual quantum constituents of semiconductor nanostructures has been widely demonstrated [4, 5, 6]. If the spatial near-field resolution falls below the extension of confined quan-

tum systems, spatially resolved PL maps out the spatial probability distribution of the wave function times the corresponding level occupation [7, 8]. The matrix elements governing the light-matter coupling are a convolution of the quantum states with the exciting electromagnetic field. This convolution implies that exciting a direct gap bulk semiconductor with a light field of a given wavevector resonant with the energy gap results in exciting excitons (i.e. bound state interband optical transitions) within the same wavevector. Succeeding in confining the optical excitation to a very small volume below the diffraction limit, implies the presence of optical fields with high lateral spatial frequencies, determining coupling matrix elements that can differ significantly from far-field ones [8, 9, 10, 11, 12, 13]. The most striking manifestation of these effects is the breaking of the usual optical selection rules and the possibility to excite dark states whose optical excitation is forbidden by symmetry in the far field. Spatial maps of dark states in semiconductor nanostructures were simulated for high-resolution SNOM in absorption and two-photon experiments [9, 14, 15, 16]. Moreover, dark states are not able to emit light in the far-field, for they generate only fields with high in-plane wavevectors corresponding to evanescent waves. Hence their lifetimes at low temperatures result significantly increased with respect to their bright counterparts.

In this letter we theoretically investigate the impact of the reduced dark-states relaxation on the distribution of electron-hole pairs among the available energy levels after a far-field continuous wave excitation. We find that this reduced relaxation significantly throws off balance the PL population dynamics resulting in striking deviations from equilibrium. In particular we find that, even at steady state, the occupation of the dark first excited state of a symmetric artificial atom can exceed that of the ground state. Usually larger populations for higher energy levels in nanosystems are observed as consequence of bottleneck

---

\*Author to whom correspondence should be addressed; electronic mail: salvatore.savasta@unime.it

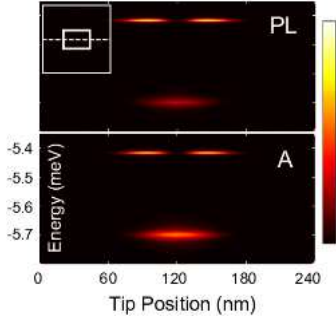


FIG. 1: (color online). (a) Near-field PL signal (collection-mode) as a function of photon energy and beam position (line scan shown in the inset) obtained under uniform illumination of the sample at the energy of the QW 1s exciton.  $T=2$  K,  $FWHM=40$  nm. (b) Total absorption under local illumination, along the same line, spatial resolution and temperature as in (a).

effects due to efficient radiative recombination occurring before relaxation to the lowest energy-levels. Here the inverted occupations origin from the opposite effect: carrier trapping due to the presence of nonradiative states. While the observation of such effects by means of far-field spectroscopy is prevented (dark states are not able to emit), a SNOM tip can collect the evanescent waves generated by the occupation of dark states. Hence near-field PL reveals to be an excellent laboratory to address general questions regarding nanoscale energy transfer in open quantum systems.

In this work we consider quantum states confined in a naturally occurring quantum dot, or terrace, induced by monolayer fluctuations in the thickness of a GaAs/AlGaAs semiconductor quantum well. We adopt the usual envelope function and assume that the electron-hole wave functions factorize into a center of mass and a relative part given by the 1s state of quantum well excitons [3]. We assume that the radiative decay of excitons is not drastically altered by the presence of the SNOM tip. As pointed out in Ref. [16], this is a reasonable assumption since the photons can be emitted into any solid-angle direction, and the slightly modified photon density of states in the presence of the SNOM tip is not expected to be of great importance. Within these assumptions, recently [8] it has been shown that the near-field spectrally resolved PL signal collected by the tip can be written as

$$I_{PL}(\bar{\mathbf{R}}_{out}, \omega_{out}) = r_0 \sum_{\alpha} |o_{\alpha}^{out}(\bar{\mathbf{R}}_{out})|^2 \mathcal{L}_{\alpha}(\omega_{out}) N_{\alpha} . \quad (1)$$

where  $o_{\alpha}^{out} = \int d^2\mathbf{R} \tilde{E}_{out}(\mathbf{R}) \psi_{\alpha}(\mathbf{R})$  is the overlap of the exciton wavefunctions with the signal mode  $\tilde{E}_{out}(\mathbf{R})$  supported by the tip centered at the position  $\bar{\mathbf{R}}_{out}$  (collection mode),  $\pi \mathcal{L}_{\alpha}(\omega) = \Gamma / [(\omega - \omega_{\alpha})^2 + \Gamma^2]$ , where  $\Gamma$  is the dephasing rate of the exciton due to radiative emission and phonon scattering. In Eq. (1)  $N_{\alpha}$  are the diagonal terms of the exciton density matrix. The kinetic equation for the diagonal terms of the exciton density matrix can

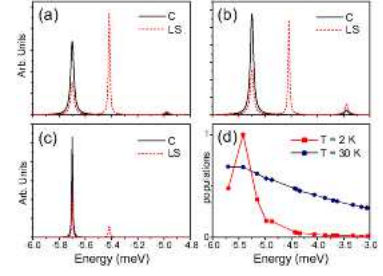


FIG. 2: (color online). (a) PL spectra obtained in collection mode ( $FWHM = 40$  nm and  $T = 4$  K). The spectra have been obtained centering the tip at one of the two emission maxima of the first excited state (LS) and at the emission maximum of the ground state (C); (b) Total absorption under local illumination obtained with spatial resolution, at temperature and centering the snom tip as in Fig. 2(a); (c) PL spectra as in Fig. 2(a) where the radiative decay rates of all the levels are set two orders of magnitude lower than the lowest nonradiative decay rate. (d) Level occupations (normalized at the maximum) calculated for two different temperatures.

be derived from the Heisenberg equations of motion for the exciton operators under the influence of the system Hamiltonian [8]. The relevant Hamiltonian is constituted by the bare electronic Hamiltonian of the semiconductor system, the interaction Hamiltonian of the semiconductor with the light field and the interaction Hamiltonian of excitons with the phonon bath. In the following we consider a low-excitation regime, and according to the dynamics controlled truncation scheme [17] we include only states with one electron-hole pair (excitons). In addition, we neglect the possible coherent phonon states and the memory effects induced by the photon and phonon fields. The resulting set of kinetic equations is [2, 3, 8]

$$\partial_t N_{\alpha} = G_{\alpha}(\omega_{in}) + \sum_{\beta} \gamma_{\alpha \leftarrow \beta} N_{\beta} - 2\Gamma_{\alpha} N_{\alpha} , \quad (2)$$

where  $\gamma_{\beta \leftarrow \alpha}$  are the phonon-assisted scattering rates.  $2\Gamma_{\alpha} = r_{\alpha} + \sum_{\beta} \gamma_{\beta \leftarrow \alpha}$  is the total out-scattering rate, being  $r_{\alpha}$  the rate for spontaneous emission, proportional to the exciton oscillator strength:  $r_{\alpha} = r_0 |\int d^2\mathbf{R} \psi_{\alpha}(\mathbf{R})|^2$ . In this equation the generation term depends on the spatial overlap between the illuminating beam and the exciton wavefunctions:  $G_{\alpha} = r_0 |o_{\alpha}^{in}|^2 \mathcal{L}_{\alpha}(\omega_{in})$  and  $o_{\alpha}^{in}$ , analogously to  $o_{\alpha}^{out}$ , contains the overlap of the exciton wavefunctions with the signal mode  $\tilde{E}_{in}(\mathbf{R})$  delivered by the tip centered at  $\bar{\mathbf{R}}_{in}$ . In collection mode (far-field illumination) the input field can be considered as uniform over the QW plane:  $\tilde{E}_{in}(\mathbf{R}) = \tilde{E}_{in}^0$ .

We apply the above developed theoretical scheme to calculate the individual occupations of exciton states confined in the dot after a continuous-wave far-field optical excitation resonant with the energy of the 1s QW exciton (the dot barrier). The obtained occupations are then used to study the spatially and spectrally resolved (collection mode) light emission from the dot. The effective potential felt by 1s excitons used in our simulations is represented by a sample of  $(240 \times 240)$  nm with a pro-

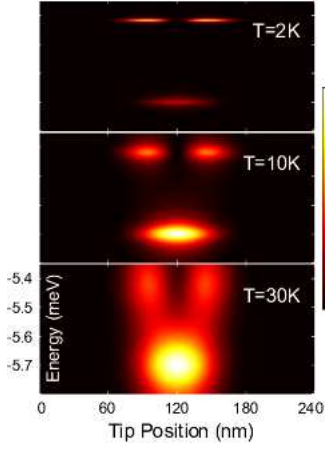


FIG. 3: (color online). PL spectral line-scans calculated at three different temperatures, with  $\text{FWHM} = 40$  nm.

typical interface-fluctuation confinement of rectangular shape with dimensions  $(60 \times 90)$  nm, and monolayer fluctuations giving rise to a 6 meV effective confinement potential. The upper panel of Fig. 1 displays the near-field PL signal as a function of photon energy and beam position obtained after uniform illumination of the sample at the energy of the 1s QW exciton in the absence of interface fluctuations, fixed as zero of energy ( $\omega_I = 0$  meV). The specific line scan is indicated in the inset. A Gaussian profile with  $\text{FWHM} = 40$  nm of the electromagnetic-mode supported by the collecting tip has been assumed. The line scan clearly evidences the first excited state of the dot which is dark under far-field collection. We observe that its spectral line is more intense and narrow (owing to the absence of radiative decay) than that of the ground state. The calculated PL spectra shows that dark-states can be observed by high-resolution SNOM in the usual collection mode configuration after nonresonant far-field excitation, without the need of nonlinear optical interactions. Analogous results are expected for locally collected electroluminescence. For comparison we plotted in the lower panel the total absorption under local illumination ( $\text{FWHM} = 40$  nm). As near-field PL is proportional to this quantity times the level occupations, the comparison provides interesting information about the steady-state exciton populations. The two panels clearly indicate that the level occupation of the dark-state is significantly larger than that of the ground state, at the opposite to what predicted by the Boltzmann distribution. The observed inverted occupations origin from symmetry-suppression of radiative decay of the dark-state and the quite small nonradiative scattering at low temperature ( $T = 2\text{K}$ ) for states well confined in the dot. This behaviour is better evidenced in panels 2(a) and 2(b). The spectra have been obtained centering the tip at one of the two emission maxima of the first excited state (LS) and at the emission maximum of the ground state (C). In order to better specify the origin of the inverted occupations, we calculated the PL spectra as in Fig. 2(a) except that we artificially

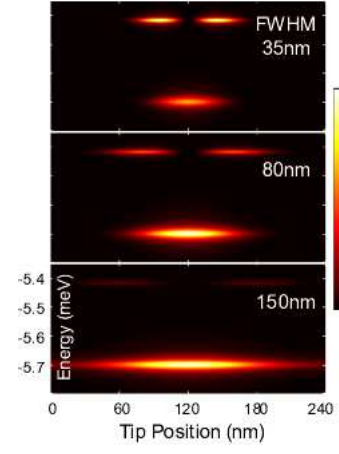


FIG. 4: (color online). PL spectral line-scans calculated at three different spatial resolutions, at the temperature of 4 K.

set the radiative decay rates of all the levels two orders of magnitude lower than the lowest nonradiative decay rate. Panel 2(c) displays the results showing that, as expected in this case, equilibrium is recovered and the near-field emission from the dot lowest energy level dominates even when the tip is centered on the maximum of the dark-state emission. Fig. 2(d) shows the calculated level occupations at  $T = 2\text{K}$  and  $T = 30\text{K}$ . At  $T = 2\text{K}$  all the occupations with the striking exception of the second energy level decrease monotonically with energy. This level displaying an occupation density which is more than a factor two that of the lowest energy level. At  $T = 30\text{K}$  the monotonous behaviour is recovered for all the energy levels. We notice that the sum of the occupations obtained at  $T = 30\text{K}$  is significantly larger than that at  $T = 2\text{K}$ . At low temperature a large fraction of the resonantly generated QW excitons (with a quite large radiative decay rate) recombine by radiative emission, while at higher temperature phonon scattering lowers this effect, increasing the carrier density captured by the dot. Fig. 3 shows the near-field ( $\text{FWHM} = 40$  nm) PL spectral line-scans obtained at three different temperatures. Increasing the temperature all states are able to better thermalize, frequently emitting and absorbing phonons before radiative emission. The influence of spatial resolution on the PL spectral line-scans is shown in Fig. 4. This figure displays the line-scans calculated at  $T = 2\text{K}$  for three different spatial resolutions (indicated in the figure). Lowering spatial resolution, the signal from the dark state tend to disappear owing to cancellation effects in the matrix element  $o_{\alpha}^{out}$  governing the light-matter coupling. Finally, we test the influence of random interface fluctuations with a correlation length of the order of the exciton Bohr-radius [2, 3]. The total effective potential felt by excitons is obtained adding to the dot potential used for all the previous calculations a contribution modeled as a zero mean, Gauss distributed and spatially correlated process with a correlation length  $\sigma = 8$  nm and a width of the energy distribution  $v_0 = 0.6$  meV (about the 10% of the dot potential-well). Fig. 5(a)

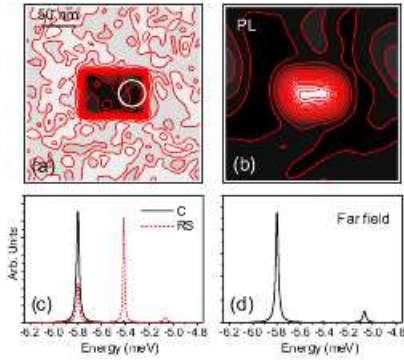


FIG. 5: (color online). (a) Specific realization of the effective disordered potential used for the calculation of the PL images and spectra show. (b) PL energy-integrated image obtained after uniform illumination of the sample at the barrier energy and collecting locally ( $FWHM = 40$  nm,  $T = 4$  K). (c) PL spectra calculated centering the tip in the center of the dot and in the position indicated by a circle in the first panel ( $FWHM = 40$  nm,  $T = 4$  K). (d) Far-field PL spectrum ( $FWHM = 40$  nm,  $T = 4$  K).

displays a specific realization of this potential. Fig. 5(b) displays the energy-integrated PL image ( $FWHM = 40$

nm,  $T = 2K$ ) for the potential realization shown in panel 5(a). It evidences the efficiency of the dot capture and near-field emission. Fig. 5(c) shows that the presence of the symmetry-breaking disordered potential slightly increases the linewidth of the second energy level, determining a slight equilibration of the emission lines. Fig. 5(d) displays the far-field PL spectrum. A very small peak (not present in the absence of disorder) appears at the energy of the second level, which thus remains mainly dark, demonstrating the robustness of dark-states with respect to this kind of disorder. Results obtained for other specific realizations of the random potential (here not shown), don't display qualitative differences.

In conclusion, we have investigated the impact of the reduced dark-states relaxation on the distribution of electron-hole pairs among the available energy levels after a far-field continuous wave excitation. The calculated near-field luminescence properties of these states depend critically on tip position, temperature and spatial resolution and clearly indicate the potentiality of near-field PL for addressing general questions regarding nanoscale energy transfer in open nanosystems.

- 
- [1] C. G. Smith, Rep. Prog. Phys. **59**, 235-282 (1996).
  - [2] R. Zimmermann *et al*, Superlattices Microstruct. **17**, 439 (1995).
  - [3] R. Zimmermann and E. Runge, Phys. Status Solidi (a) **164**, 511 (1997).
  - [4] H. F. Hess, E. Betzig, T. D. Harris, L. N. Pfeiffer, and K. W. West, Science **264**, 1740 (1994).
  - [5] J. R. Guest, T. Hstievater, Gang Chen, E. A. Tabak, B. GÖrr, D. G. Steel, D. Gammon, and D. S. Katzer, Science **293**, 2224 (2001).
  - [6] K. Matsuda *et al*, Phys. Rev. Lett. **91**, 177401 (2003).
  - [7] E. Runge, C. Lineau, Appl. Phys. B **84**, 103110 (2006).
  - [8] G. Pistone, S. Savasta, O. Di Stefano, and R. Girlanda, Appl. Phys. Lett. **84**, 2971 (2004).
  - [9] O. Mauritz, G. Goldoni, F. Rossi, and E. Molinari, Phys. Rev. Lett. **82**, 847 (1999).
  - [10] O. Di Stefano, S. Savasta, G. Martino, and R. Girlanda, Appl. Phys. Lett. **77**, 2804 (2000).
  - [11] O. Di Stefano, S. Savasta, and R. Girlanda, J. Appl. Phys. **91**, 2302 (2002).
  - [12] G. Pistone, S. Savasta, O. Di Stefano, and R. Girlanda, Phys. Rev. B **67**, 153305 (2003).
  - [13] G. Martino, G. Pistone, S. Savasta, O. Di Stefano, and R. Girlanda, J. Phys.: Condens. Matter **18**, 2367 (2006).
  - [14] O. Di Stefano, S. Savasta, G. Martino, and R. Girlanda, Phys. Rev. B **62**, 11071 (2000).
  - [15] U. Hohenester, G. Goldoni, and E. Molinari, Appl. Phys. Lett. **84**, 3963 (2004).
  - [16] U. Hohenester, G. Goldoni, and E. Molinari, Phys. Rev. Lett. **95**, 216802 (2005).
  - [17] V. M. Axt, K. Victor, and A. Stahl, Phys. Rev. B **53**, 7244 (1996).